

The energy relaxation of a nonlinear oscillator coupled to a linear bath

Joel S. Bader, B. J. Berne, Eli Pollak, and Peter Hänggi

Citation: *The Journal of Chemical Physics* **104**, 1111 (1996); doi: 10.1063/1.470766

View online: <http://dx.doi.org/10.1063/1.470766>

View Table of Contents: <http://scitation.aip.org/content/aip/journal/jcp/104/3?ver=pdfcov>

Published by the [AIP Publishing](#)

Articles you may be interested in

[Vibrational spectroscopy and relaxation of an anharmonic oscillator coupled to harmonic bath](#)

J. Chem. Phys. **134**, 204511 (2011); 10.1063/1.3594093

[Return to equilibrium for an anharmonic oscillator coupled to a heat bath](#)

J. Math. Phys. **52**, 022110 (2011); 10.1063/1.3544476

[Two-dimensional Raman and infrared vibrational spectroscopy for a harmonic oscillator system nonlinearly coupled with a colored noise bath](#)

J. Chem. Phys. **120**, 260 (2004); 10.1063/1.1629272

[Vibrational spectroscopy of a harmonic oscillator system nonlinearly coupled to a heat bath](#)

J. Chem. Phys. **117**, 6221 (2002); 10.1063/1.1503778

[Exactly Solvable Nonlinear Relaxation Processes. Systems of Coupled Harmonic Oscillators](#)

J. Chem. Phys. **45**, 1105 (1966); 10.1063/1.1727722



The energy relaxation of a nonlinear oscillator coupled to a linear bath

Joel S. Bader^{a)}

Department of Chemistry, Columbia University, New York, New York 10027

B. J. Berne^{b)}

Institute of Physics, University of Augsburg, Memminger Str. 6, D-86135 Augsburg, Germany

Eli Pollak

Chemical Physics Department, The Weizmann Institute of Science, 76100 Rehovot, Israel

Peter Hänggi

Lehrstuhl für Theoretische Physik I, Universität Augsburg, D-86135 Augsburg, Germany

(Received 2 June 1995; accepted 26 July 1995)

We develop an expression for the rate of energy relaxation of a nonlinear oscillator coupled to a linear, dissipative bath. This particular type of model has wide applicability to studies of relaxation rates of vibrational modes in chemical systems. The energy relaxation rate is estimated by relating the anharmonic oscillator to an effective harmonic reference system. The theoretical predictions compare favorably with simulation results for the energy relaxation of a Morse oscillator (i) coupled to an Ohmic bath and (ii) coupled to a bath with exponentially decaying friction. The dependence of the initial relaxation rate on the excitation energy of a Morse oscillator is qualitatively different for the two cases. When the oscillator is coupled to an Ohmic bath, the initial relaxation rate decreases as a function of the excitation energy. When exponentially decaying friction is employed, however, the initial relaxation rate is an increasing function of the excitation energy. © 1995 American Institute of Physics. [S0021-9606(95)00541-X]

I. INTRODUCTION

A vibrationally excited molecule in the presence of a thermal bath of other molecules will eventually come to equilibrium by losing energy to the bath. The rate of energy loss can serve as a probe of intramolecular couplings and intermolecular interactions. Consequently, relaxation rates for particular systems can vary over many orders of magnitude. In a real molecular solvent, energy relaxation depends on the strength of the coupling between a vibrationally excited molecule and the surrounding solvent. Furthermore, in order for there to be effective energy transfer, there must be a frequency match between the solute vibrations and the solvent modes. This resonance condition between the tagged excited mode and the solvent modes can cause a wide variation in vibrational relaxation rates in different systems.

Early theoretical models have represented the excited solute vibrational mode as a harmonic oscillator, and the solvent modes as a collection of harmonic oscillators. The dynamics generated by such a model are equivalent to a generalized Langevin equation (GLE) with time-dependent friction. The resonance condition between the solute and solvent becomes clear through a perturbation theory estimate for the vibrational relaxation rate. This rate can be extracted from the Fourier transform of the friction kernel of the bath, taken at the frequency of the excited oscillator.¹⁻⁸ The same general form for the relaxation rate is obtained for a quantum

mechanical oscillator coupled to a quantum mechanical bath.⁹⁻¹⁴ Indeed, if the oscillator and bath modes are harmonic and the coupling is bilinear, both a classical and a quantum treatment lead to the same prediction for the relaxation rate.¹⁵

A noteworthy limitation of the theoretical treatment outlined is that the solute mode is assumed to be harmonic. In reality, molecular vibrations are anharmonic, and the anharmonicity becomes increasingly important as higher energies are probed. Thus the instantaneous frequency of an anharmonic oscillator can depend sensitively on the instantaneous oscillator energy. As an excited oscillator relaxes, the instantaneous frequency can slide in and out of resonance with solvent modes.^{16,17} The result is that there is no longer a single rate describing the vibrational relaxation, but rather a dynamically changing rate which depends on the instantaneous energy.

Molecular dynamics simulations have demonstrated this effect. Early workers, stimulated by experimental results for the photolysis, geminate recombination, and vibrational relaxation of I₂ in CCl₄,¹⁸ noted a stagnation effect in the relaxation of I₂ and Br₂ in simple fluids^{19,20} and in Ar clusters.¹⁷ More recently, Tuckerman and Berne have performed molecular dynamics simulations of a diatomic molecule with an internal Morse potential in a fluid of Lennard-Jones particles.⁸ They found that the relaxation rate was very dependent on the excitation energy. They were also able to extract a friction kernel from the full molecular dynamics, and to use the friction kernel in a stochastic GLE simulation. The GLE dynamics successfully reproduced the energy relaxation from molecular dynamics. This indicates that the GLE friction kernel accurately represents the full molecular

^{a)}Permanent address: CuraGen Corporation, 322 East Main Street, Branford, Connecticut 06405.

^{b)}Permanent address: Department of Chemistry, Columbia University, New York, New York 10027.

solvent. The GLE can be considered an intermediate step between a molecular dynamics simulation and a theoretical prediction for the relaxation rate. Although the GLE itself performed well, Tuckerman and Berne noted that a linear response estimate of the relaxation rate, based on the GLE friction kernel and on motion close to the bottom of the Morse potential, was a poor predictor of the relaxation.

We focus here on extending the theoretical treatment for a harmonic oscillator to understand the relaxation of an anharmonic oscillator coupled to a dissipative bath in the context of GLE dynamics. The frequency of an anharmonic oscillator depends on its energy, and consequently it changes throughout the relaxation. We develop in Sec. II a perturbation theory prediction for the energy relaxation rate. This prediction is based on a harmonic reference system which depends on the instantaneous energy of the anharmonic oscillator through the oscillator action $J(E)$. In Sec. III, the theoretical predictions are discussed along with results from trajectories obtained by simulations of the full GLE dynamics.

A striking feature predicted by the theory and evident in the simulation results is the qualitative difference for relaxation of a Morse oscillator due to Ohmic friction and relaxation due to memory friction. In the case of Ohmic friction, we find that the energy relaxation rate is faster the lower the energy. Conversely, for memory friction the relaxation rate can be faster the higher the energy. This difference provides an immediate experimental criterion to judge whether or not memory friction is important, and is discussed in greater depth in the conclusion, Sec. IV.

II. THEORY

The system considered here consists of an oscillator coupled linearly to a dissipative bath. The coupling of the oscillator to the bath is described by a generalized Langevin equation, which includes a frictional damping and a stochastic force,

$$\mu \ddot{q}(t) = -\frac{\partial}{\partial q} V(q) - \int_0^t dt' \zeta(t-t') \dot{q}(t') + \xi(t). \quad (1)$$

The effective mass of the oscillator q is μ , the bare potential is $V(q)$, and the stochastic force $\xi(t)$ is related to the friction kernel $\zeta(t)$ by the fluctuation–dissipation theorem,

$$\zeta(t) = \beta \langle \xi(t) \xi(0) \rangle. \quad (2)$$

The thermal energy β^{-1} is $k_B T$. It is convenient to define the Fourier–Laplace transform of $\zeta(t)/\mu$ as

$$\tilde{\gamma}'(\omega) + i \tilde{\gamma}''(\omega) = \int_0^\infty dt e^{i\omega t} \zeta(t)/\mu. \quad (3)$$

The energy of the oscillator is defined as

$$E = V(q) + \frac{1}{2} \mu \dot{q}^2. \quad (4)$$

We suppose that at $t=0$ the oscillator is placed in a high energy state, $E \gg k_B T$. We also assume that the potential $V(q)$ is harmonic for energies around $k_B T$. The form of the GLE then requires that $\langle E(t) \rangle \rightarrow k_B T$ as $t \rightarrow \infty$, where the

average implies a sampling over random force histories $\xi(t)$. In the remainder of this section, we develop a theoretical prediction for the relaxation of $E(t)$ back to equilibrium. We restrict attention to the case of weak frictional damping. A practical definition for weak damping is that the oscillator undergoes many periods of motion before losing energy on the order of $k_B T$.

We suppose that the potential $V(q)$ corresponds to purely harmonic motion,

$$V(q) = \frac{1}{2} \mu \omega_0^2 q^2. \quad (5)$$

The condition of weak damping implies that $\omega_0 \gg \tilde{\gamma}'(\omega_0)$.⁸ When this condition is satisfied, perturbation theory predicts that

$$\frac{\langle E(t) - k_B T \rangle_{E(0)}}{E(0) - k_B T} = \exp[-t/T_1], \quad (6)$$

with $T_1^{-1} = \tilde{\gamma}'(\omega_0)$.⁸ The average is over random force histories, and the subscript indicates that the initial energy of the oscillator is $E(0)$.

This expression can be obtained as follows. First, we assume that the oscillator initially has energy E with a period of $T(E)$. The average energy change of the oscillator over a period is defined as $\Delta(E)$. We also assume that the potential is harmonic, $V(q) = \frac{1}{2} \mu \omega_0^2 q^2$. Averaging over random force histories and dispensing with the angle brackets, it can be shown that^{21,22}

$$\Delta(E) = -\tilde{\gamma}'(\omega_0)[J(E) - J_{\text{eq}}]. \quad (7)$$

The action of the oscillator at energy E is $J(E)$,

$$J(E) = \oint p dq, \quad (8)$$

and the integral is over the orbit of energy E . The term J_{eq} is the average action at equilibrium, or $J(k_B T)$.

At this point we generalize the perturbation theory to an anharmonic oscillator. For an anharmonic oscillator at energy E , it is possible to define an effective instantaneous frequency from the relationship

$$T(E) = \frac{2\pi}{\omega(E)} = \frac{dJ(E)}{dE}. \quad (9)$$

We use the effective frequency $\omega(E)$ and the action $J(E)$ to define a harmonic reference system. The frequency of the harmonic reference system is $\omega_0 = \omega(E)$ and the action of the harmonic reference is chosen to reproduce the value of the action of the anharmonic system. This implies that the energy of the harmonic system, equal to $\omega(E)J(E)/2\pi$, can be different from E , the energy of the anharmonic system.

We assume that the harmonic reference system, defined by $J(E)$ and $\omega(E)$, can be used to estimate the energy loss of the anharmonic oscillator. The change in the average energy is then

$$\frac{dE}{dt} = \Delta(E)/T(E) \quad (10a)$$

$$= -\tilde{\gamma}'(\omega(E))[J(E) - J_{\text{eq}}]/[dJ(E)/dE] \quad (10b)$$

$$= -\tilde{\gamma}'(\omega(E))dE/d \ln[J(E) - J_{\text{eq}}]. \quad (10c)$$

A derivation of Eq. (10a) may be found in the Appendix. Thus we find for the relaxation of the action the equation

$$(d/dt)\ln[J(E) - J_{\text{eq}}] = -\tilde{\gamma}'(\omega(E)). \quad (10d)$$

The frequency $\omega(E)$ can also be written in terms of the action as $\omega(J) = 2\pi dE(J)/dJ$, allowing the energy loss equation to be expressed entirely in terms of the action $J(t)$ and J_{eq} :

$$(d/dt)\ln[J - J_{\text{eq}}] = -\tilde{\gamma}'[\omega(J)]. \quad (10e)$$

In these equations, the action $J(E)$ has taken on the meaning of $J(\langle E(t) \rangle)$. The initial relaxation rate immediately following an excitation to energy E is defined as

$$\text{initial rate} \equiv \frac{\Delta(E)}{(E - k_B T)T(E)}. \quad (11)$$

If the friction is Ohmic, $\tilde{\gamma}'(\omega) = \gamma_0$, and the time decay of the action is particularly simple: $J(t) - J_{\text{eq}} = [J(0) - J_{\text{eq}}]e^{-\gamma_0 t}$, where $J(0)$ is $J(E(0))$ and $J(t)$ is $J(\langle E(t) \rangle)$. We have the interesting result that, for an anharmonic oscillator, the decay of the action is purely exponential. The energy relaxation, however, is no longer exponential, unless $E(J)$ is linear in J , i.e., unless the oscillator is harmonic. To obtain the energy relaxation in the general case, one must insert $J(t)$ into the appropriate expression for $E(J)$ to obtain $\langle E(t) \rangle$.

For example, let us consider a Morse oscillator with dissociation energy D_0 ,

$$V(q) = D_0(1 - e^{-\alpha q})^2. \quad (12a)$$

The frequency for small oscillations about $q=0$ is $\omega_0 = \alpha\sqrt{2D_0}/\mu$. The period $T(E) = (2\pi/\omega_0)/\sqrt{1 - E/D_0}$ for E smaller than the dissociation energy. One finds that

$$E = (\omega_0/2\pi)J(1 - \chi J), \quad (12b)$$

with the anharmonicity parameter $\chi = \omega_0/(8\pi D_0)$. The classical anharmonicity parameter χ can be related to the quantum mechanical anharmonicity parameter χ_e , which determines the quantized energy levels $\{E_n\}$ for the Morse oscillator,

$$E_n = (n + 1/2)\hbar\omega_0 - \chi_e(n + 1/2)^2\hbar\omega. \quad (12c)$$

Using the correspondence $(n + 1/2) \rightarrow J/2\pi\hbar$, one finds that $\chi = \chi_e/2\pi\hbar$.

Returning to Eq. (12b), and defining $\Delta J = J(0) - J_{\text{eq}}$, we find for Ohmic friction that

$$E(t) = (\omega_0/2\pi)[J_{\text{eq}} + \Delta J e^{-\gamma t}][1 - \chi(J_{\text{eq}} + \Delta J e^{-\gamma t})]. \quad (12d)$$

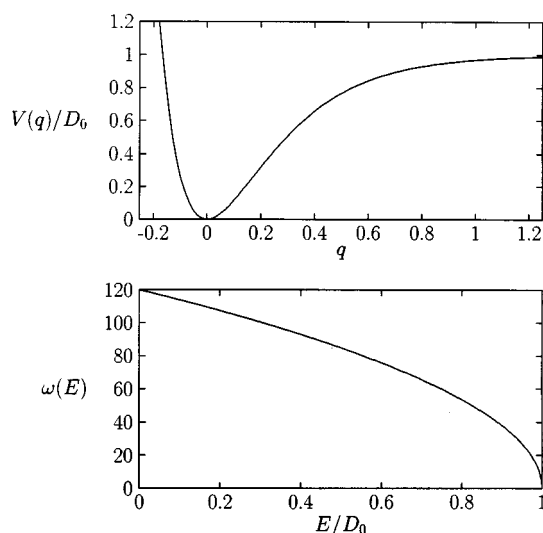


FIG. 1. The Morse potential $V(q) = D_0(1 - e^{-\alpha q})^2$ is shown for parameters $D_0 = 207.36$, $\alpha = 4.167$, and $k_B T = 2.5$. The local frequency of the oscillator, $\omega(E) = \omega_0\sqrt{1 - E/D_0}$, is shown in the bottom panel.

For exponential friction with decay time τ , one obtains $\tilde{\gamma}'(\omega) = \gamma/(1 + \omega^2\tau^2)$. The frequency $\omega(J)$ is found using Eqs. (9) and (12b) to be $\omega_0(1 - 2\chi J)$. In this case the action can be computed by integrating the equation

$$(d/dt)\ln[J(t) - J_{\text{eq}}] = -\gamma/[1 + \tau^2\omega_0^2(1 - 2\chi J)^2] \quad (12e)$$

to obtain $J(t)$. Then $\langle E(t) \rangle = (\omega_0/2\pi)J(t)(1 - \chi J(t))$.

In practice, it is a simple matter to integrate Eq. (10a) directly. Furthermore, it is not necessary to have an analytic functional form to represent $\zeta(t)$ and $\tilde{\gamma}'(\omega)$. This is of particular relevance to molecular dynamics studies, which produce numerical results for $\zeta(t)$. All that is necessary for integrating Eq. (10a) is a table of values for $\tilde{\gamma}'(\omega)$.

III. RESULTS AND DISCUSSION

To test the theory presented in the previous section, we have performed computer simulations for the energy relaxation of a Morse oscillator coupled to a frictional bath. The parameters of the Morse oscillator were selected to match those used in an earlier study.⁸ In the earlier study reduced units were used to characterize the dynamical friction and the Morse oscillator. The dynamical friction on the vibrational displacement was calculated in a Lennard-Jones fluid with potential parameters ϵ and σ . Thus one defines the reduced temperature $T^* = k_B T/\epsilon$, the reduced bond length $r^* = r/\sigma$, the reduced time $t^* = (\epsilon/m\sigma^2)^{1/2}t$, and the reduced frequency $\omega^* = (m\sigma^2/\epsilon)^{1/2}\omega$. In these units the dissociation energy was $D_0 = 207.36$ with $T^* = 2.5$. The Morse oscillator consisted of two Lennard-Jones balls with reduced mass $m^* = 1$ coupled by a Morse potential, giving the oscillator the reduced mass $\mu^* = 1/2$. The length scale parameter α for the Morse potential was chosen to be 4.167. This yields a value of 120 for the harmonic frequency ω_0 . The anharmonicity parameter then equals $\chi = 0.023$. A plot of the potential is shown in the top panel of Fig. 1. In the bottom panel of the

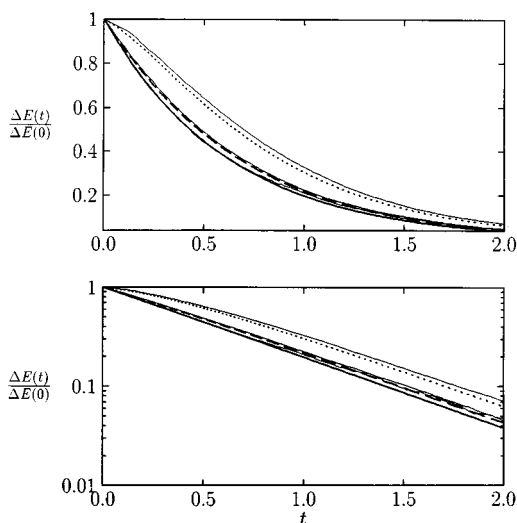


FIG. 2. The predicted energy relaxation of the Morse oscillator with $V(q)$ given in Fig. 1 and Ohmic friction $\gamma=1.65$ is shown for three initial energies: $10 k_B T$ (solid line), $40 k_B T$ (dashed line), and $80 k_B T$ (dotted line). Simulation results are shown as thin solid lines. In the bottom panel, the results are shown on a logarithmic scale.

figure, the frequency of the oscillator is shown as a function of the energy. The frequency and action are

$$\omega(E) = \omega_0 \sqrt{1 - E/D_0} \quad \text{and} \quad (13)$$

$$J(E) = (4\pi D_0 / \omega_0) [1 - \sqrt{1 - (E/D_0)}] \quad (14)$$

as functions of the energy E .

We now relate the reduced units of the simulation to the physical parameters corresponding to liquid argon. The Lennard-Jones parameters for liquid argon are $\epsilon/k_B \approx 120$ K and $\sigma \approx 3.4$ Å.²³ Thus the reduced temperature $T^* = 1/2$ corresponds to $T = 300$ K and the length scale parameter $\alpha = 4.167$ corresponds to a distance of 14.2 Å. The reduced unit of time t^* is then equivalent to 2.15 ps, and ω^* corresponds to a frequency of $0.465/\text{ps}$ or 2.47 cm^{-1} . Therefore, the reduced frequency of 120 corresponds to 296 cm^{-1} . The anharmonicity parameter χ corresponds to $6.46 \times 10^{30}/\text{Js}$, giving $\chi_e = 0.0043$.

A. Ohmic friction

Results of simulations using Ohmic friction are shown in Fig. 2. A single choice was made for the Ohmic friction parameter, $\gamma=1.65$. Three initial energies were used, $E=10, 40$, and $80 k_B T$. For each choice of initial energy, 1000 trajectories were run. Each trajectory was initiated at $q=0$ with a positive velocity $\dot{q} = \sqrt{2E/\mu}$. The integration time step was 0.001 , or about $1/50$ of the period of oscillation near the bottom of the well. The simulation results are used to judge theoretical predictions obtained by integration of Eq. (10a) for the rate of energy loss. The relaxation is characterized by $\Delta E(t)/\Delta E(0)$, where $\Delta E(t) = \langle E(t) - k_B T \rangle_{E(0)}$ and the average is over 1000 histories of the ran-

TABLE I. Instantaneous energy relaxation rates.

E_0	Energy relaxation rates ^{a,b,c}			
	Ohmic friction		Exponential friction	
	Simulation	Theory	Simulation	Theory
$10 k_B T$	1.62_4	1.60	2.6_1	1.81
$40 k_B T$	1.34_3	1.38	2.9_1	2.58
$80 k_B T$	0.48_1	0.52	2.5_2	7.17

^aThe rates are given in units of inverse reduced time, $1/t^*$.

^bThe theoretical prediction for the instantaneous relaxation rate is given by Eq. (11).

^cThe uncertainty in the last digit of the simulation results is indicated by the subscript value, i.e., 1.62_4 indicates 1.62 ± 0.04 .

dom force with the initial energy of the oscillator set to $E(0)$. The term $\Delta E(0)$ is the initial deviation from equilibrium, $E(0) - k_B T$.

For the smallest value of the initial energy, $E=10 k_B T$, the theory and simulation results agree very well. Motion at this low energy is described accurately by a harmonic reference system, for which the theoretical predictions are exact. At the next higher energy, $E=40 k_B T$, the theoretical prediction is still quite good. At the highest energy, $E=80 k_B T$, the theoretical prediction notably deviates from the simulation results. The theory predicts that the system relaxes slightly faster than is seen to occur in the simulations. At $t=1$, for instance, the theoretical prediction for the energy relaxation is that $\Delta E(t)/\Delta E(0)=0.30$, whereas a value of 0.32 is measured in the simulation, i.e. the error amounts to approximately 6%.

It is clear from Fig. 2 that the lowest energy excitation, $E=10 k_B T$, relaxes most quickly in terms of the decay of $\Delta E(t)/\Delta E(0)$, and that the highest energy excitation, $E=80 k_B T$, relaxes the slowest. The initial relaxation rates have been computed from the simulation data in Fig. 2 at early time by fitting an exponential decay to the simulation data for $t < 0.12$. We find that the initial decay rate for $E=10 k_B T$ is 1.62 ± 0.04 ; the decay rate for $E=40 k_B T$ is 1.34 ± 0.03 , and the decay rate for $E=80 k_B T$ is 0.48 ± 0.01 . The rates have been computed in units of inverse reduced time, $1/t^*$ and are summarized in Table I. The values predicted for the relaxation by Eq. (11) are seen to be quite accurate.

As seen from Eq. (11), the energy relaxation rate for an oscillator with instantaneous energy E depends on the ratio $[J(E) - J_{\text{eq}}]/T(E)$. This is because, over a period $T(E)$, the energy loss $\Delta(E) = \gamma[J(E) - J_{\text{eq}}]$, and γ is constant for Ohmic friction. For simplicity, we neglect the constant term J_{eq} in the subsequent analysis, and normalize the rate of energy loss by the instantaneous energy E . The instantaneous ratio $J(E)/[ET(E)] = 2(D_0/E)[\sqrt{1 - E/D_0} - (1 - E/D_0)]$ is shown in the top panel of Fig. 3. A single relaxation rate cannot be defined; instead, the instantaneous rate is strongly dependent on the instantaneous energy E . The behavior of the relaxation rate is due to a competition between $J(E)$ and

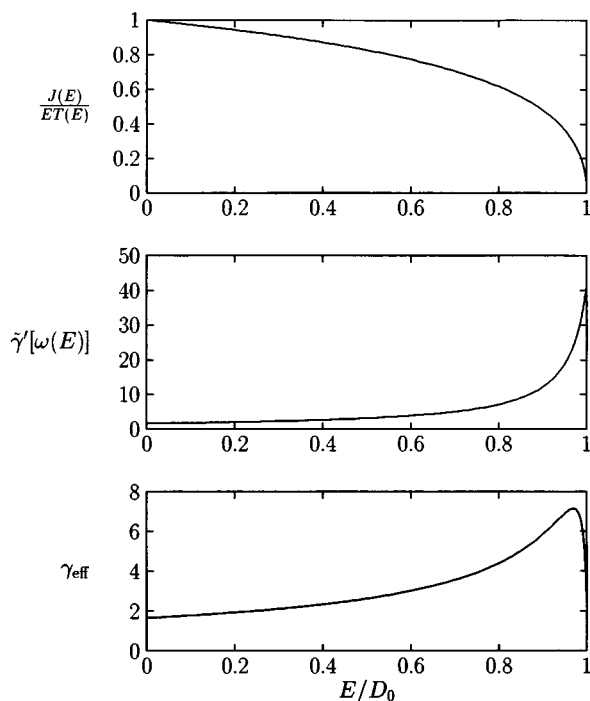


FIG. 3. The relaxation rate of a Morse oscillator coupled to Ohmic friction is determined by the ratio $J(E)/ET(E) = (2D_0/E) [\sqrt{1-E/D_0} - (1-E/D_0)]$ (top panel) and by the density of bath modes $\tilde{\gamma}'[\omega(E)]$ (middle panel). The overall relaxation rate γ_{eff} (bottom panel) is equal to the product of these two quantities, and is shown for the parameters we have used in simulations with exponential friction.

$T(E)$. As energy increases, $J(E)$ and $T(E)$ both increase. The period (which diverges as $E \rightarrow D_0$) increases more rapidly than the action and has the dominant effect.

It is interesting to note that even though the energy loss per period can be substantial, the perturbation theory for the energy relaxation rate is accurate. For example, at the largest energy we examined, $E(0) = 80 k_B T$, the energy loss per period is approximately $14 k_B T$. The perturbation theory still works because the actual perturbation parameter is not the energy loss per period but rather the ratio $\gamma/\omega(E)$ of the static friction to the instantaneous frequency of the oscillator. At low solute energies, $\omega(E) \approx \omega_0 = 120$, and $\gamma/\omega(E) \approx 0.014$, which is quite small. In fact, for the perturbation parameter to be as large as 0.1, i.e., for $\gamma/\omega(E) > 0.1$, the energy must be 98% of the dissociation energy, in this case greater than $81.4 k_B T$. The largest energy we explored, $80 k_B T$, corresponds to a perturbation parameter of 0.073.

B. Exponential friction

We have also performed simulations using exponential friction, $\gamma(t) = (\gamma_0/\tau) \exp(-t/\tau)$. For this form of friction, $\tilde{\gamma}'(\omega) = \gamma_0/(1 + \omega^2 \tau^2)$. We used the parameters $\tau = 0.04122$ and $\gamma_0 = 42$, both expressed in terms of the reduced time t^* . With this choice of parameters, $\tilde{\gamma}'(\omega_0) = 1.65$ for $\omega_0 = 120$. Note that the effective friction for this frequency was chosen to reproduce the static friction of the previous section.

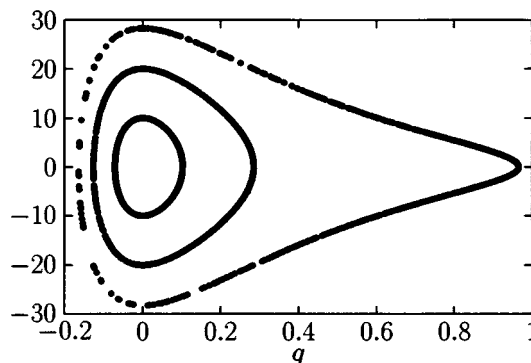


FIG. 4. The initial phase points of the Morse oscillator are shown for simulations with three different initial energies: $10 k_B T$ (inner circle), $40 k_B T$ (middle circle), and $80 k_B T$ (outer circle). For clarity, only 1000 phase points are shown for each set, although 10 000 initial phase points were used in each of the three sets to produce 10 000 independent trajectories per set.

At first, simulations were performed exactly as for the Ohmic friction case, with each trajectory starting at the phase point with initial $q=0$ and initial \dot{q} positive. As expected, this method produced reproducible oscillations in the energy decay. To remove the oscillations and thus simplify the analysis, we performed a second set of simulations in which the initial phase point was chosen at random for each trajectory. Only data from the second set of simulations are presented here.

For a given initial energy $E(0)$, the initial phase point for each trajectory was chosen randomly and uniformly on the microcanonical surface for $E=E(0)$. To accomplish this, we selected a random time t_{random} from a uniform distribution between times 0 and $T[E(0)]$, the period for undamped motion at energy $E(0)$. The initial q and \dot{q} were then determined by propagating the undamped motion from the inner turning point for a time t_{random} . This propagation can be performed analytically; in this case, however, the propagation was performed numerically. To ensure proper averaging, 10 000 phase points were selected at random for each of the three initial energies, $E(0) = 10 k_B T$, $40 k_B T$, and $80 k_B T$. These initial phase points are depicted in Fig. 4. For clarity, only 1000 of each of the 10 000 phase points are shown for each of the three initial energies. The inner ring corresponds to the lowest energy, $10 k_B T$, and the outer ring corresponds to the highest energy, $80 k_B T$.

The simulation results for $\Delta E(t)/\Delta E(0)$ for the three initial energies 10, 40, and $80 k_B T$ are shown in Fig. 5. Also shown are the relaxation predictions from Eq. (10a). In the top panel of the figure, the relaxation is shown on a regular axis, and in the bottom panel the relaxation is shown on a semi-logarithmic axis. The gross features of the relaxation, common to both the theoretical predictions (thick lines, dashes, and dots) and the simulation results (thin lines) are evident in these plots.

First, the results depicted in Fig. 5 demonstrate that (after a short transient period) the overall relaxation rate increases with increasing excitation energy. The relaxation is slowest for the smallest excitation energy ($E = 10 k_B T$, thick line), and is fastest for the largest excitation energy ($E = 80$

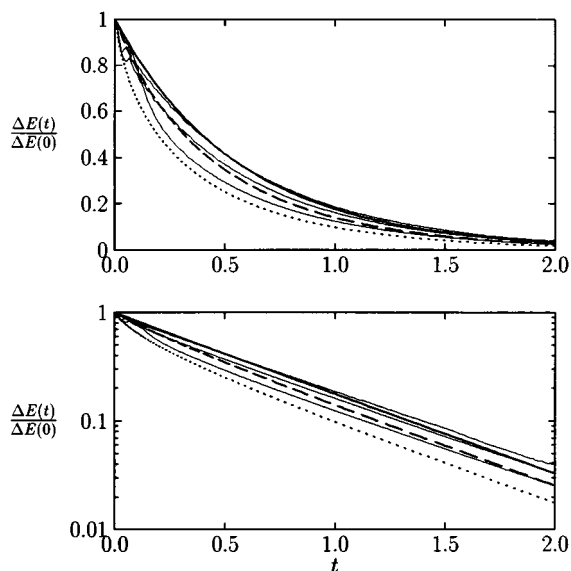


FIG. 5. The predicted energy relaxation of the Morse oscillator with $V(q)$ given in Fig. 1 and exponential friction is shown for three initial energies: $10 k_B T$ (solid line), $40 k_B T$ (dashed line), and $80 k_B T$ (dotted line). Simulation results are shown as thin solid lines. In the bottom panel, the results are shown on a logarithmic scale. In the simulations, 10 000 trajectories with randomly chosen initial phase contributed for each of the three energies.

$k_B T$, dotted line). In this respect, the theoretical predictions agree with the simulation results. According to the theory, the relaxation rate for a given oscillator energy E is directly proportional to the product of two factors. The first factor, $J(E)/ET(E)$, measures the dependence of the oscillator action on the oscillator energy. For a harmonic oscillator, this quantity is unity. For the Morse oscillator, this quantity is equal to $(2/x)[\sqrt{1-x} - (1-x)]$, where $x = E/D_0$ (the ratio of the oscillator energy to the dissociation energy), and is shown in the top panel of Fig. 3. The first factor therefore decreases as the energy decreases, therefore favoring a slower relaxation rate as the oscillator energy increases (as was seen with Ohmic friction).

This effect is outweighed, however, by the behavior of the second factor, the component of the friction $\tilde{\gamma}'(\omega)$ evaluated at the local frequency $\omega(E)$ corresponding to the oscillator energy. The quantity $\tilde{\gamma}'(\omega)$ is depicted in the middle panel of Fig. 3 as a function of the oscillator energy E . It is clear that this second factor is an increasing function of the oscillator energy. At larger energies, the oscillator frequency decreases, and the friction has a larger component at a lower frequency.

The overall relaxation rate is the product of the two factors described above, and it is depicted in the bottom panel of Fig. 3. The frequency-dependent behavior of $\tilde{\gamma}'(\omega)$ is clearly the dominant effect in determining the frequency dependence of the relaxation rate. The relaxation rate is seen to increase with oscillator energy for all but the highest energies. Of course, at very high energies, the oscillator period diverges and the relaxation rate goes to zero. This creates a turnover in the relaxation rate for energies very close to the dissociation energy D_0 . To lowest order in $1/(\omega_0 \tau)^2$, where

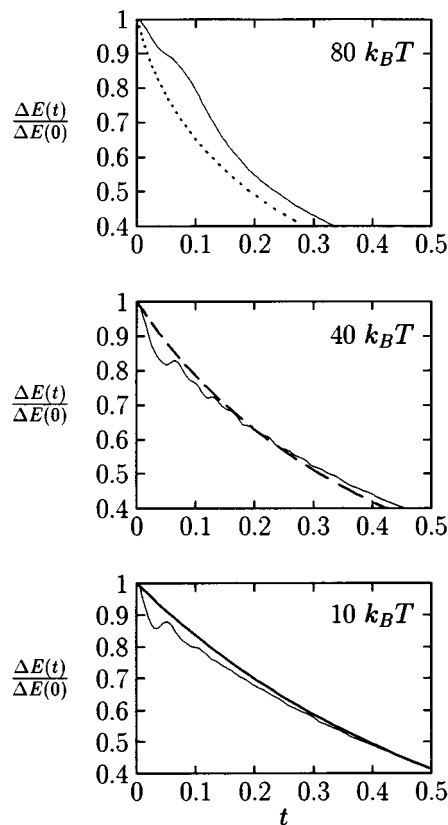


FIG. 6. The early-time results in Fig. 5 for a Morse oscillator with $V(q)$ given in Fig. 1, coupled to an exponential-friction bath, are shown for three initial energies: $10 k_B T$ (bottom panel), $40 k_B T$ (middle panel), and $80 k_B T$ (top panel). Simulation results are shown as thin solid lines.

ω_0 is the oscillator frequency at the bottom of the well and τ is the decay time of the exponential friction, the turnover occurs at $E/D_0 = 1/(\omega_0 \tau)^2$, or 0.959 for the parameters we have chosen. This low-order estimate is very close to the actual location of the turnover, $E/D_0 = 0.9697$, or $E = 80.43 k_B T$.

After an early transient period, the overall energy relaxation predicted by the theory is faster than is seen in the simulations in Fig. 5. The same type of systematic error was observed in the previous section dealing with Ohmic friction, but the error is larger here. The reason that the overall discrepancy is larger for memory friction than for static friction is most likely because the perturbation parameter is becoming larger. The effective perturbation parameter is $\gamma_0/\omega(E)$, where γ_0 is the full damping (rather than the component of the friction at the oscillator frequency, which is smaller). In our simulations, the perturbation parameter for energies close to $k_B T$ is 0.35, and the parameter increases as the excitation energy increases. The perturbation theory also fails to predict the early-time oscillations in the energy relaxation. These oscillations are shown in greater detail in Fig. 6, along with the theoretical predictions. Other than the lack of oscillations, the general agreement between theory and simulation is quite good for the two lower energies.

The perturbation theory for the energy loss embodied in Eq. (10a) is incapable of predicting the oscillations in the

decay because it involves only a first derivative of the energy with respect to time. A higher-order perturbation theory, involving higher-order derivatives, would be required to obtain such oscillations. The exact result for the energy relaxation of a harmonic oscillator coupled to an exponential bath does show oscillations, and we present such results below. First, however, we compare the initial rate of energy loss predicted by the theory to that observed in the simulations.

For purposes of comparison, the envelope of the energy decay from the simulation is used to determine the initial rate of energy loss. Thus, the initial energy rate from the simulation is defined as

$$\text{initial rate} = -(1/t_1) \ln[\Delta E(t_1)/\Delta E(0)], \quad (15)$$

where t_1 is the maximum for the first oscillation. The relaxation using the largest initial energy, $E=80 k_B T$, did not produce an oscillation large enough to yield a maximum in the energy decay. In this case the initial rate was estimated by an exponential fit to the simulation data for $t < 0.1$. The rates from the simulation are 2.6 ± 0.1 for $E=10 k_B T$, 2.9 ± 0.1 for $E=40 k_B T$, and 2.5 ± 0.2 for $E=80 k_B T$. The rates from the theory are, respectively, 1.81, 2.58, and 7.17. These rates are summarized, along with the results from Ohmic friction, in Table I. Unlike the theoretical prediction, the initial rate of energy decay is not a monotonically increasing function of the initial energy. The initial rate increases from $E=10 k_B T$ to $40 k_B T$, then decreases from $40 k_B T$ to $80 k_B T$. It is likely that the perturbation theory is failing at the highest energy of the Morse oscillator due to the extreme anharmonicity at this energy. The initial rate from perturbation theory is 30% too small at the lowest energy, and 10% too small at the middle energy.

We now return to an investigation of the oscillations in the energy decay. Oscillations arise in the energy relaxation of a harmonic oscillator coupled to an exponential bath due to the different correlation functions involving q and \dot{q} in Eq. (16) being out of phase with each other. When the initial energy of an oscillator of frequency ω_0 is selected from a microcanonical ensemble, one can show that the energy relaxation is

$$\Delta E(t)/\Delta E(0) = (1/2)C_{qq}^2(t) + (1/2)C_{\dot{q}\dot{q}}^2(t) + (1/\omega_0^2)\dot{C}_{qq}^2(t), \quad (16)$$

where $C_{qq}(t)$ and $C_{\dot{q}\dot{q}}(t)$ are, respectively, the normalized correlation functions $\langle q(t)q(0) \rangle / \langle q^2 \rangle$ and $\langle \dot{q}(t)\dot{q}(0) \rangle / \langle \dot{q}^2 \rangle$.⁸ The Laplace transforms of these correlation functions are simple to express in terms of $D(s) = s^2 + s\tilde{\gamma}(s) + \omega_0^2$:

$$\tilde{C}_{qq}(s) = [s + \tilde{\gamma}(s)]/D(s), \quad (17)$$

$$\tilde{C}_{\dot{q}\dot{q}}(s) = -\omega_0^2/D(s), \quad (18)$$

$$\tilde{\dot{C}}_{qq}(s) = s/D(s). \quad (19)$$

When the friction kernel is exponential, performing the inverse Laplace transform reduces to obtaining the roots of a cubic polynomial. These roots can be obtained analytically from a well-known formula.²⁴

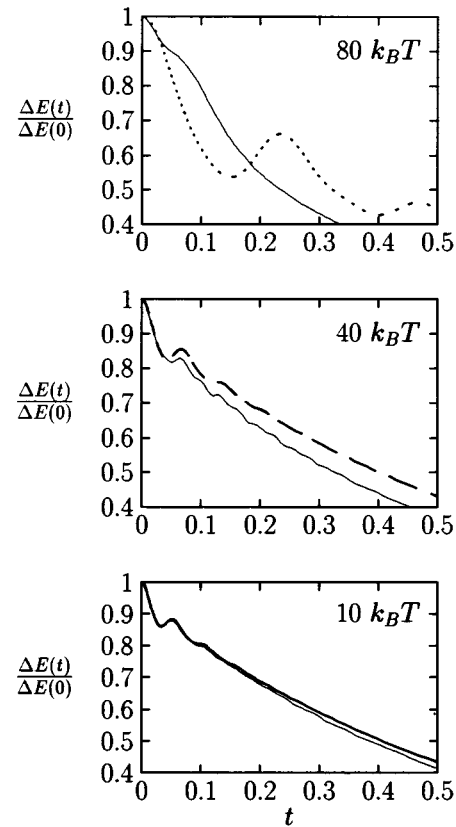


FIG. 7. The predicted energy relaxation of the Morse oscillator with $V(q)$ given in Fig. 1 and exponential friction is shown for three initial energies: $10 k_B T$ (bottom panel), $40 k_B T$ (middle panel), and $80 k_B T$ (top panel). Simulation results are shown as thin solid lines. The thick curves are predicted from the correlation function $\langle q(t)q(0) \rangle$ based on the initial value of the oscillator frequency, $\omega(E_0)$.

In the top panel of Fig. 7 the early-time simulation results are compared with this theory for the energy relaxation using $\omega[E(0)]$ for the frequency of the harmonic oscillator. The three roots required for the inverse Laplace transform are listed in Table II. For the lowest energy, $E(0)=10 k_B T$, the theory does quite well in predicting the oscillations in the energy relaxation. This good agreement is to be expected since anharmonicities are negligible for this low an excitation energy. For the next larger excitation energy, $E(0)=40 k_B T$, the correlation function theory predicts an oscillation in the energy relaxation at the same time that the oscillation occurs in the simulation results. For the highest energy, $E(0)=80 k_B T$, this theory predicts oscillations much larger than those seen in the simulations.

Although the correlation-function based theory describes the early-time oscillations in energy relaxation, it fails to

TABLE II. Roots needed for the inverse Laplace transform.

$E(0)$	Roots
$10 k_B T$	$-21.21, -0.7726 \pm 116.6i$
$40 k_B T$	$-15.94, -0.7579 \pm 90.35i$
$80 k_B T$	$-3.342, -0.6142 \pm 26.43i$

describe the relaxation properly for longer times. The discrepancy is quite evident for the early-time results depicted in Fig. 7 and continues to grow for longer times. This is especially true for the largest initial energy, $E(0) = 80 k_B T$.

IV. CONCLUSION

As opposed to the relaxation of a harmonic oscillator coupled to a dissipative bath, for which the energy relaxation rate is independent of the excitation energy, the energy relaxation rate of an anharmonic oscillator does depend on the excitation energy. We have developed a simple theory for determining the relaxation rate of an anharmonic oscillator. The theory relates the anharmonic oscillator to an effective harmonic oscillator chosen to have the same action $J(E)$ and frequency $\omega(E)$ for the instantaneous value of the energy E . We find that the theoretical prediction performs well in comparison to simulation results for a Morse oscillator.

The theory we have developed predicts a striking qualitative difference for relaxation due to coupling to Ohmic friction, and for relaxation due to coupling to memory friction. For Ohmic friction, the relaxation rate decreases as the excitation energy increases. This is because the instantaneous rate of energy loss is proportional to $J(E)/T(E)$. The action $J(E)$ changes slowly as the energy E approaches the dissociation energy, whereas the period $T(E)$ diverges in the same limit.

Conversely, for exponential friction (or other appropriate dissipative baths), the relaxation rate can increase with increasing energy. The relaxation rate for memory friction is dependent on the density of bath modes at the oscillator frequency. The qualitative picture is that of a dynamically changing solute frequency which slides in and out of resonance with bath modes.^{16,17} The spectrum of bath modes is often largest at low frequencies commensurate with the rattling of solvent atoms adjacent to a solute. The effective frequency of a Morse oscillator decreases as its energy increases, allowing it to couple more effectively with these low frequency solvent modes, and increasing the rate of energy relaxation.

The perturbation theory described here is incapable of producing the expected oscillations in the energy relaxation which arise naturally when even a purely harmonic oscillator is coupled to a bath with memory friction. The oscillations are predicted very well by a separate perturbation theory for the autocorrelation function $\langle q(t)q(0) \rangle$ for an appropriate reference system. In our implementation, the reference system was based on the Morse oscillator at its initial energy. Because we did not allow the reference system to adjust to the instantaneous energy of the oscillator, the energy relaxation predicted according to $\langle q(t)q(0) \rangle$ was only correct at early times. It is not too difficult to imagine an improved perturbation theory in which the reference system is allowed to implicitly adjust as the oscillator loses energy to the bath. In light of the excellent early-time results depicted in Fig. 7, such a perturbation theory would no doubt provide nearly quantitative agreement with simulation results.

The theoretical results obtained here are based on the

framework of GLE dynamics. Our theory accounts for the frequency of an excited mode sliding in and out of resonance with modes in a bath represented by a GLE friction kernel. Thus the validity of our approach is probably limited to systems for which the GLE is a good approximation for the solvent friction, and for which the perturbation theory for the energy loss is reasonable. For memory friction, the perturbation parameter is proportional to the full damping (rather than the component of the damping at the solute frequency). Thus, the perturbation parameter for memory friction can be large even when the actual energy loss is small, leading to errors in the perturbation theory and in the predicted relaxation. It is easy to envision a PGH-type coordinate transformation which would correct for this problem with the perturbation theory.²¹ It would also be possible to introduce corrections due to space and time dependent friction.^{24,25} To account for space dependence, the energy loss expression, Eq. (7) would be modified to include an integration of the space dependence. In this case, the energy loss would no longer be directly related to the action.

We find a systematic error in the theoretical predictions, namely that the predicted relaxation rate is slightly too large. However, in light of the simplicity of the harmonic reference system, it is important to note that the systematic error is quite small.

ACKNOWLEDGMENTS

This work was supported by a grant from the National Science Foundation (B.J.B) and by the Alexander von Humboldt Foundation (B.J.B). We thank Professor Gregory Voth for very useful comments on microcanonical sampling.

APPENDIX: DERIVATION OF THE ENERGY LOSS $\Delta(E)$

The rate of change of the energy $E = V(q) + \frac{1}{2}\mu\dot{q}^2$ is

$$\begin{aligned} \frac{dE(t)}{dt} &= \frac{dV(q)}{dq} \dot{q}(t) + \mu\dot{q}(t)\ddot{q}(t) \\ &= \dot{q}(t) \left[- \int_0^t dt' \gamma(t-t') \mu\dot{q}(t') + \xi(t) \right]. \end{aligned} \quad (\text{A1})$$

The second equation follows from the definition of the GLE, Eq. (1). We neglect $\xi(t)$ for the moment and concentrate on the energy dissipation. The energy loss per period, $\Delta(E)$, is

$$\begin{aligned} \Delta(E) &= \int_0^{T(E)} dt \frac{dE}{dt} \\ &= - \int_0^{T(E)} dt \dot{q}(t) \int_0^t dt' \gamma(t-t') \mu\dot{q}(t'), \end{aligned} \quad (\text{A2})$$

where $T(E) = 2\pi/\omega(E)$ is the period of the anharmonic oscillator at energy E .

We can find the energy loss $\Delta(E)$ to the lowest order in the damping by inserting into Eq. (A2) the trajectory $q_0(t)$ corresponding to the undamped harmonic reference system,

$$q_0(t) = \sqrt{J(E)/\pi\mu\omega(E)}\cos(\omega(E)t). \quad (\text{A3})$$

The energy loss, to lowest order in the damping $\gamma(t)$, is

$$\Delta(E) = -\frac{\omega(E)J(E)}{\pi} \int_0^{T(E)} dt \sin(\omega(E)t) \times \int_{-\infty}^t dt' \gamma(t-t') \sin(\omega(E)t'). \quad (\text{A4})$$

Extending the limit on the second integral to $-\infty$ is appropriate when the decay of $\gamma(t)$ is fast relative to the period $T(E)$. It should also be appropriate to extend the limit of the integral when the period $T(E)$ is fast relative to the time required to lose $k_B T$ of energy. The second integral can be expressed as $\sin(\omega(E)t)\tilde{\gamma}'(\omega(E)) - \cos(\omega(E)t)\tilde{\gamma}''(\omega(E))$. Using the orthogonality of $\sin(\omega(E)t)$ and $\cos(\omega(E)t)$ over the period $T(E)$, we find that

$$\Delta(E) = -J(E)\tilde{\gamma}'(\omega(E)). \quad (\text{A5})$$

This equation implies that energy is dissipated until $J(E)=0$, i.e., until all the energy has been dissipated from the oscillator into the bath. In reality, one expects dissipation to continue until the oscillator has attained thermal equilibrium with an energy on the order of $k_B T$.

When terms involving the random force $\xi(t)$ are retained in the calculation of $\Delta(E)$, the oscillator is found to gain energy back from the bath. This can be seen by expressing the velocity $\dot{q}(t)$ as $\dot{q}_0(t) + \delta\dot{q}(t)$, where $\dot{q}_0(t)$ is the velocity of the undamped reference trajectory. To lowest order in the perturbation due to the frictional bath,

$$\delta\dot{q}(t) = \int_{-\infty}^t dt' \mu^{-1} \xi(t'). \quad (\text{A6})$$

Note that terms involving the friction kernel $\zeta(t)$ are of higher order and do not appear. Inserting this expression for $\delta\dot{q}(t)$ into Eq. (A2), we find an energy gain per period which on average is

$$\int_0^{T(E)} dt \int_{-\infty}^t dt' \mu^{-1} \langle \xi(t)\xi(t') \rangle = k_B T \tilde{\gamma}'(0) T(E). \quad (\text{A7})$$

We note that this perturbation theory for the energy gain per period is not entirely correct. First, our low order expansion for $\delta\dot{q}(t)$ implies that all the bath modes are capable of

driving the oscillator coordinate. Actually, only those bath modes resonant with the oscillator are capable of driving its motion, which suggests the substitution $\tilde{\gamma}'(0) \rightarrow \tilde{\gamma}'(\omega(E))$. Furthermore, the low order perturbation theory has a secular divergence when $T(E)$ becomes large. However, for a harmonic reference system, we have the relationship $T(E) = J(E)/E$, which suggests an energy gain per period of $\tilde{\gamma}'(\omega(E))J(E)k_B T/E$. Furthermore, for a harmonic reference, $J(E)k_B T/E = J(k_B T) \equiv J_{\text{eq}}$, which provides the expression we used for the energy loss per period:

$$\Delta(E) = -\tilde{\gamma}'(\omega(E))[J(E) - J_{\text{eq}}]. \quad (\text{A8})$$

For energies larger than $k_B T$, the oscillator loses energy to the frictional bath; for energies smaller than $k_B T$, the oscillator gains energy from the bath.

¹R. Kubo, *Fluctuations, Relaxation, and Resonance in Magnetic Systems*, edited by D. Ter Haar (Plenum, New York, 1962).

²R. Kubo, *Adv. Chem. Phys.* **13**, 101 (1963).

³R. Kubo, *J. Math. Phys.* **4**, 174 (1963).

⁴R. Zwanzig, *J. Stat. Phys.* **9**, 215 (1973).

⁵A. M. Levine, M. Shapiro, and E. Pollak, *J. Chem. Phys.* **88**, 1959 (1988).

⁶R. M. Whitnell, K. R. Wilson, and J. T. Hynes, *J. Phys. Chem.* **94**, 8625 (1990).

⁷R. M. Whitnell, K. R. Wilson, and J. T. Hynes, *J. Chem. Phys.* **96**, 5354 (1992).

⁸M. Tuckerman and B. J. Berne, *J. Chem. Phys.* **98**, 7301 (1993).

⁹A. G. Redfield, *IBM J. Res. Dev.* **1**, 19 (1957).

¹⁰R. Zwanzig, *J. Chem. Phys.* **34**, 1931 (1961).

¹¹D. W. Oxtoby, *Adv. Chem. Phys.* **40**, 1 (1979).

¹²D. W. Oxtoby, *Adv. Chem. Phys.* **47**, 487 (1981).

¹³F. E. Figueirido and R. M. Levy, *J. Chem. Phys.* **97**, 703 (1992).

¹⁴H. Gai and G. A. Voth, *J. Chem. Phys.* **99**, 740 (1993).

¹⁵J. S. Bader and B. J. Berne, *J. Chem. Phys.* **100**, 8359 (1994).

¹⁶I. E. L. Sibert, W. P. Reinhardt, and J. T. Hynes, *Chem. Phys. Lett.* **42**, 455 (1982).

¹⁷F. G. Amar and B. J. Berne, *J. Phys. Chem.* **88**, 6720 (1984).

¹⁸T. J. Chuang, G. W. Hoffman, and K. B. Eisenthal, *Chem. Phys. Lett.* **25**, 201 (1974).

¹⁹P. Bado, P. H. Berens, and K. R. Wilson, *Proc. SPIE* **322**, 230 (1982).

²⁰D. J. Nesbitt and J. T. Hynes, *J. Chem. Phys.* **77**, 2130 (1982).

²¹E. Pollak, H. Grabert, and P. Hänggi, *J. Chem. Phys.* **91**, 4073 (1989).

²²J. S. Bader, B. J. Berne, and E. Pollak, *J. Chem. Phys.* (in press).

²³M. P. Allen and D. J. Tildesley, *Computer Simulation of Liquids* (Oxford University, New York, 1987).

²⁴*Handbook of Chemistry and Physics*, edited by R. C. Weast (Chemical Rubber, Boca Raton, 1987).

²⁵J. B. Straus, J. M. Gomez-Llorente, and G. A. Voth, *J. Chem. Phys.* **98**, 4082 (1993).

²⁶G. R. Haynes, G. A. Voth, and E. Pollak, *J. Chem. Phys.* **101**, 7811 (1994).